Statistics of energy flows in spring-coupled one-dimensional subsystems

By C. S. Manohar and A. J. Keane

University of Oxford, Department of Engineering Science, Parks Road, Oxford OX1 3PJ, U.K.

This paper considers the problem of determining the statistical fluctuations occurring in the vibrational energy flow characteristics of a system of two multimodal, random, one-dimensional subsystems coupled through a spring and subject to single frequency forcing. The subsystems are modelled either as transversely vibrating Euler–Bernoulli beams or as axially vibrating rods. The masses of the subsystems are modelled as random variables. The calculations of energy flows are based on an exact formulation which uses the Green functions of the uncoupled subsystems, which, in turn, are expressed as summations over the uncoupled modes. Factors influencing the number of modes contributing to the response statistics at any specified driving frequency are investigated. A criterion for identifying the driving frequency beyond which the mean power spectra become smooth is proposed. Empirical procedures are developed to predict the 5% and 95% probability points given knowledge of the first two moments of the response. The work reported here forms part of a long term study into the reliability of statistical energy analysis (SEA) methods.

1. Introduction

The process of averaging in statistical energy analysis (SEA) is carried out for two main reasons: first, it accounts for the random nature of the forces exerted on most structures, thereby simplifying measures of response; and second, it caters for the stochastic modelling of the system which is adopted to allow for the sensitivity of high-frequency responses to minor changes in physical and modelling parameters. It must also be noted that the primary response variables of interest in SEA are the steady state average total energies stored in the subsystems. These quantities are obtained as integrals over the extent of the subsystems and also over driving frequency bands, which imply a further combination of both spatial and frequency averaging. The results obtained are clearly dependent on details of the averaging processes such as the frequency bandwidths, quantities treated as random and the probability distribution functions assumed for these random quantities. Each form of averaging is accompanied by a reduction in the resolution of the response with respect to amplitude, time, space or frequency parameters. This is, of course, consistent with the primary aim of SEA modelling, which is to produce simplified models of system behaviour which describe gross properties of system responses. However, in order that the average results can be interpreted properly, especially with respect to observations made on a single realization of a system or an excitation over a limited time or frequency interval, it is essential that each process of averaging be accompanied by associated estimates of the measures of dispersion. While it is fairly straightforward to analyse the dispersion associated with averaging across an

Phil. Trans. R. Soc. Lond. A (1994) **346**, 525–542
Printed in Great Britain

ensemble of time histories using standard random vibration theory (see Lin 1967), the study of other forms of averaging is considerably more complicated. This difficulty constitutes a major shortcoming in the application of SEA procedures to practical problems and has received relatively little attention in the literature. Work has so far been carried out in this direction by Lyon & Eichler (1964), Lyon (1969), Davies & Wahab (1981), Davies & Khandoker (1982), Fahy & Mohammed (1992) and Keane & Manohar (1993). The studies conducted by Skudrzyk (1968, 1980, 1987) on the bounds of system transfer functions can also be cited in this context. A discussion on related issues can also be found in the works of Scharton & Lyon (1968), Hodges & Woodhouse (1986), Heron (1990) and Craik (1991).

The present study considers this problem by investigating the stochastic variability of energy flows in a system of coupled beams or rods. The statistics of the dissipated powers in the individual subsystems are investigated as functions of driving frequency, for the cases of point harmonic and rain-on-the-roof type distributed excitations (i.e. for single frequency driving). The bands enclosing the 5% and 95% probability points are shown to display different types of behaviours, namely, oscillatory, convergent, divergent or stationary, depending on the choice of subsystem type (i.e. beams or rods), damping models, type of excitation and details of the stochastic model used for the system. A non-dimensional parameter related to the variability in the subsystem natural frequencies is introduced which is shown to be useful in characterizing the frequency beyond which the resonant behaviour of individual modes no longer dominates the response statistics. Clearly, this frequency represents a cutoff point below which simplified theories like SEA cannot be guaranteed to work well. The problem of estimating confidence bands empirically using knowledge of the first two moments is also investigated. This study shows that the energy flow statistics can be described reasonably well using either gamma or lognormal probability distribution functions.

2. The two-subsystem model

The system under consideration consists of a pair of transversely vibrating beams or axially vibrating rods, which are mutually coupled through a spring, the system configuration being illustrated in figure 1. The subsystems are assumed to have random material and/or geometrical properties and are taken to be viscously damped. No restrictions are placed either on the magnitude of damping or the strength of the coupling spring. The external excitations acting on the system are modelled either as point harmonic forces or as a rain-on-the-roof type distributed forcing. The aim of the present study is to examine the probabilistic nature of the energy flow characteristics in the system arising out of random fluctuations in the system properties. The deterministic aspects of energy flow characteristics in this type of system have been studied by Davies (1973) and Keane (1992). The expressions for the receptance functions and the input, dissipated and coupling powers are readily available in these references and hence are reproduced here without detailed derivation. Thus, when two subsystems are coupled at $x_i = a_i$ and excited by point forces $F_i(t)$ acting at $x_i = b_i, i = 1, 2$, the input power and coupling power receptances for the first subsystem are given respectively by

$$H_{\mathrm{in}\,1}(\omega) = (\omega^2/m_1) \sum_{i=1}^{\infty} c_{1i}(\psi_i(b_1)/|\phi_i|^2) + (\omega k_c/m_1^2)\,\mathrm{Im}\left\{\frac{1}{\Delta}\left[\sum_{i=1}^{\infty} \psi_i(b_1)\,\psi_i(a_1)/\phi_i\right]^2\right\} \quad (1)$$

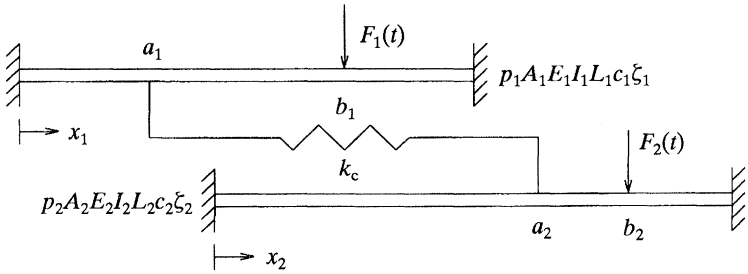

Figure 1. Two spring coupled one-dimensional subsystems.

and
$$H_{12}(\omega) = \frac{\omega^2 k_c^2}{m_1^2 m_2 |\Delta|^2} \sum_{r=1}^{\infty} c_{2r}(\psi_r^2(a_2)/|\phi_r|^2) \left| \sum_{i=1}^{\infty} (\psi_i(b_1)\psi_i(a_1)/\phi_i) \right|^2. \tag{2}$$

Similarly, when the system is excited by distributed forces $F_i(x_i, t), i = 1, 2$, of the rain-on-the-roof type, the above receptances are given by

$$H_{in1}(\omega) = (\omega^2/m_1) \sum_{i=1}^{\infty} c_{1i}(1/|\phi_i|^2) + (\omega k_c/m_1^2) \operatorname{Im}\left\{ \sum_{i=1}^{\infty} (\psi_i^2(a_1)/\phi_i^2 \Delta) \right\} \tag{3}$$

and
$$H_{12}(\omega) = \frac{\omega^2 k_c^2}{m_1^2 m_2 |\Delta|^2} \sum_{r=1}^{\infty} c_{2r}(\psi_r(a_2)/|\phi_r|^2) \sum_{i=1}^{\infty} (\psi_i^2(a_1)/|\phi_i|^2). \tag{4}$$

In these equations the summations over the indices i and r respectively denote summations over the modes of the first and second subsystems. The quantities ω_i and ψ_i are the natural frequencies and mode shapes with the quantities ϕ_i and Δ given by

$$\phi_i = \omega_i^2 - \omega^2 + i c_{1i}\omega \quad \text{and} \quad \Delta = 1 + (k_c/m_1) \sum_{i=1}^{\infty} (\psi_i^2(a_1)/\phi_i) + (k_c/m_2) \sum_{r=1}^{\infty} (\psi_r^2(a_2)/\phi_r). \tag{5, 6}$$

The mode shapes ψ satisfy the orthogonality conditions given by

$$\int \psi_i(x_1)\psi_j(x_1)\rho_1(x_1)\,\mathrm{d}x_1 = m_1 \delta_{ij}. \tag{7}$$

Here δ_{ij} denotes the Kronecker delta function. The quantities m_i and ρ_i denote the total mass and mass per unit length of the ith subsystem. c_{ij} is the damping coefficient of the ith subsystem in the jth mode; k_c is the coupling spring constant. The forces F_1 and F_2 are assumed to be ergodic and statistically independent. The spectra of the input, coupling and dissipated powers can be related using the above receptance functions as follows:

$$\Pi_{in1}(\omega) = H_{in1}(\omega) S_{F_1}(\omega), \quad \Pi_{12}(\omega) = H_{12}(\omega) S_{F_1}(\omega) - H_{21}(\omega) S_{F_2}(\omega) \tag{8, 9}$$

and
$$\Pi_{diss1}(\omega) = \Pi_{in1}(\omega) - \Pi_{12}(\omega). \tag{10}$$

Here $S_{F_i}(\omega)$ is the power auto-spectral density function of $F_i(t)$.

When the mass and/or stiffness properties of the individual subsystems are modelled as random quantities, the natural frequencies and mode shapes become random in nature. The functions described above, in turn, become random processes. The aim of the present investigation is to obtain probabilistic descriptions of the different power functions given in equations (8)–(10) as functions of the probabilistic descriptions of the masses of the individual rods. Estimates for the probability

distribution functions (PDFs) of these quantities can currently only be obtained using Monte Carlo simulation techniques. For this purpose, an ensemble of realizations of coupled subsystems are computationally simulated as per the stochastic model adopted. For every realization of the pairs of subsystems, the natural frequencies and mode shapes are calculated for the individual subsystems and this information incorporated into equations (1)–(4) to generate the ensemble of receptance functions. This ensemble is further processes to obtain the desired PDFs.

For simple theories like SEA to be useful, it is clearly necessary that the mean spectra of the different power functions become stationary with increases in the frequency of interest and moreover, the 5% and 95% probability points should preferably converge towards the mean. For any given problem it is not obvious at the outset whether such behaviour occurs and this study identifies some of the more influential factors.

3. Modal overlap and statistical overlap factors

The receptance functions and power spectra have been expressed in equations (1)–(10) in terms of summations over the modes of the uncoupled subsystems. At any specified frequency, the number of modes making significant contributions to the response is clearly dependent on the bandwidth of the nearby modes and the modal frequency spacing. The ratio of these two quantities has been defined in the literature as the modal overlap factor, see Lyon (1975). The modal spacing is governed by the type of subsystem considered; for example, it remains constant with frequency for axially vibrating rods and increases linearly for transversely vibrating Euler–Bernoulli beams. The modal bandwidth, on the other hand, is a function of the damping model adopted for the subsystem. In SEA studies the damping is normally taken to be viscous and proportional. Within the framework of this assumption several alternatives are possible which can dramatically alter the behaviour of the receptances and power spectra. Thus, if the damping force per unit length is expressed as $r(x)\,\dot{y}(x,t)$, the damping coefficient $r(x)$ can be taken to be proportional to local mass, stiffness or a linear combination of mass and stiffness. Depending on the model used, the modal damping factor, ζ_n, can either fall or rise with the mode count n. Another alternative which is commonly employed, is to take ζ_n to be a constant for all modes. In this study the damping is taken to be either mass proportional, leading to modal damping factors falling with frequency and constant modal bandwidths, B_n, or to be represented by constant damping factors. These two damping models are summarized in table 1 where the relevant expressions for simply supported beams and fixed–fixed rods are given. It may be observed from the table that for constant B_n, the model overlap factor remains fixed for rods while it varies as n^{-1} for beams; conversely for constant ζ_n, the overlap factor varies as n for both beams and rods.

It should be noted here that the strength of random fluctuation assumed for the subsystem mass parameters has a significant effect on the number of modes contributing to the statistics of the spectra at any specified frequency. In order to see this, consider subsystems in which the mass per unit length ρ is uniform and modelled as

$$\rho = \rho_0(1+\epsilon U), \tag{11}$$

where U is a gaussian random variable with zero mean and unit standard deviation and ϵ controls the degree of randomness. Figure 2 shows the resulting probability

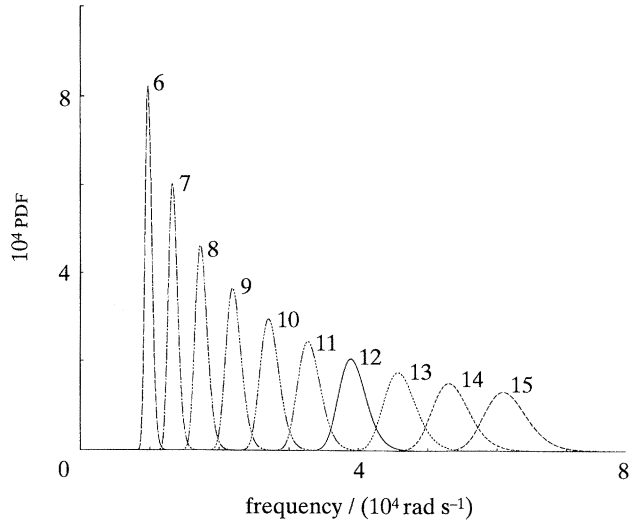

Figure 2. Probability density functions for natural frequencies of beam 1; $\epsilon = 0.10$. Values of n as indicated on figure.

Table 1. *Modal properties of rods and beams*

quantity	B_n	ζ_n	beam	rod
natural frequency	—	—	$n^2\pi^2/L^2\sqrt{(EI/\rho)}$	$n\pi/L\sqrt{(AE/\rho)}$
modal spacing	—	—	$\pi^2/L^2(1+2n)\sqrt{(EI/\rho)}$	$\pi/L\sqrt{(AE/\rho)}$
modal overlap factor, M	c	$c/2\omega_n$	$cL^2/\pi^2(1+2n)\langle\sqrt{(EI/\rho)}\rangle$	$cL/\pi\langle\sqrt{(AE/\rho)}\rangle$
	$2\zeta\omega_n$	ζ	$2\zeta n^2/1+2n$	$2\zeta n$
statistical overlap factor, S_n	—	—	$2\beta n^2/1+2n$	$2\alpha n$

$$M = \frac{\text{mean modal bandwidth}}{\text{mean modal spacing}}, \quad S_n = \frac{2\sigma_n}{\langle\omega_{n+1}-\omega_n\rangle},$$

$$\alpha = \sqrt{[\langle AE/\rho\rangle - \langle\sqrt{(AE/\rho)}\rangle^2]}/\langle\sqrt{(AE/\rho)}\rangle, \quad \beta = \sqrt{[\langle EI/\rho\rangle - \langle\sqrt{(EI/\rho)}\rangle^2]}/\langle\sqrt{(EI/\rho)}\rangle.$$

density functions of a set of ten consecutive natural frequencies for a simply supported beam (a similar plot is obtained for the case of a fixed–fixed rod, except that the frequency spacing is then constant). It can be seen from this figure that the probability density functions 'overlap' increasingly for higher frequencies. This overlap will clearly be greater for larger ϵ. This implies that the randomness parameter ϵ plays a role similar to that of the damping bandwidth in the sense that, at any specified frequency, an increase in ϵ results in a larger number of modes contributing to the *statistics* of the response. This behaviour is not reflected clearly in the definition of the model overlap factor although it is weakly dependent on ϵ. Consequently, it is useful to introduce a statistical overlap factor defined by

$$S_n = 2\sigma_n/\langle\omega_{n+1}-\omega_n\rangle, \tag{12}$$

where σ_n is the standard deviation of the nth natural frequency. From table 1 it can be seen that this overlap factor increases as n for both rods and beams. As will be seen in the later sections, S_n can be shown to be related to the frequency beyond which the oscillations in the *statistics* of the power spectra die out. It may be noted that this quantity is closely related to the 'spacing signal to noise ratio' discussed by Soong & Bogdanoff (1963) in the context of simple oscillator chains, where departures from the expected values of natural frequencies were studied.

4. Statistics of response power spectra

The factors likely to influence the number of modes contributing to responses at any specified frequency have been discussed in the previous section. The results of a parametric survey on the statistics of the response power spectra are presented in this section, highlighting the role played by these factors. The study of such response statistics is currently not feasible using analytical procedures and here numerical simulation methods have been used. There are three main questions of interest which this survey attempts to address.

1. Under what conditions do the ensemble mean square responses become stationary with respect to the driving frequency?

2. If they do, what is the frequency beyond which this behaviour can be expected to occur?

3. Do the contours of 5% and 95% probability points converge onto the mean, become constant or diverge, with increases in driving frequency?

Various factors pertaining to subsystem type, damping, stochastic modelling, excitation and strength of coupling can be expected to influence the answers to these questions. Of these, the consequences of the stochastic model employed for the subsystems are perhaps the most difficult to predict. In an earlier study we considered the energy flow characteristics in a system of two coupled, axially vibrating stochastic rods and examined different types of random system models (Keane & Manohar 1993). For most, but not all types of randomness, the transfer functions were shown to become stationary above certain values of driving frequency; equation (11) being of this type. The present study is not focused on the details of different randomization schemes and so this model is adopted throughout. None the less, failure to exhibit stationarity should not be discounted when attempting to apply SEA methods.

The remaining factors of interest have been studied by carrying out a full survey based on the system of two coupled subsystems already illustrated in figure 1; table 2 details the subsystem properties used. The effects of varying various parameters in the problem were considered as follows: subsystem type (Euler–Bernoulli beams or axially vibrating rods), damping models (constant modal bandwidth or constant modal damping coefficient), magnitude of damping (see table 3), levels of system randomness ($\epsilon = 0.01$, 0.05 or 0.10) and type of excitation (point harmonic or distributed rain-on-the-roof excitation). It may be observed from table 3 that the parameter values for the two damping models have been chosen so that the 10th mode of rod vibration and 4th mode of beam vibration both have identical damping factors and modal bandwidths for subsystem 1; these modes lying 25% of the way through the frequencies considered here. Throughout this survey the energies dissipated in the two subsystems were investigated for the case when the first subsystem was excited by external forces with the second subsystem driven only indirectly through the coupling spring. Consequently, the power dissipated in the undriven subsystem is proportional to the cross power receptance function while that dissipated in the driven subsystem reflects both the input and cross power receptances, see again equations (8)–(10). The coupling spring constants were chosen as $k_c = 0.9 \times 10^9$ N m^{-1} for the rod systems and $k_c = 0.1 \times 10^9$ N m^{-1} for the beam systems to ensure that the subsystems were well coupled to each other (i.e. so that the behaviour of the undriven subsystem significantly affects that of the driven one (see Keane 1992)). An excitation frequency range from 0 to 50000 rad s^{-1} was

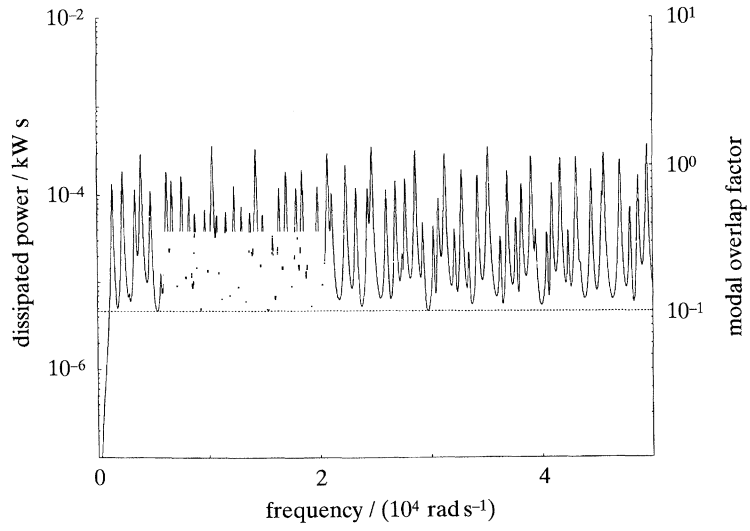

Figure 3. Dissipated power spectral density function for subsystem 1 of the rod system; rain-on-the-roof excitation; $c = 130\ s^{-1}$. ——, power; · · · · · ·, modal overlap factor.

Table 2. *Subsystem physical properties*

subsystem	length/m	rigidity	mass/unit length (kg m^{-1})	drive point, a/m	coupling point, b/m
rod 1	5.0	17.85 MN	4.156	1.15	3.15
rod 2	4.5	17.85 MN	4.156	—	2.115
beam 1	1.0	1536.5 N m^2	2.0141	0.23	0.63
beam 2	0.9	1536.5 N m^2	2.0141	—	0.423

Table 3. *Subsystem damping properties*

(Rod 2 and beam 2 have equivalent values of B_n and ζ_n.)

system	bandwidth	damping coefficient
rod 1	$B_1 = 13.0,\ B_{10} = 130.2,\ B_{40} = 520.8$	$\zeta_n = 0.005$
	$B_1 = 78.1,\ B_{10} = 781.2,\ B_{40} = 3124.8$	$\zeta_n = 0.03$
	$B_n = 130.0$	$\zeta_1 = 0.05,\ \zeta_{10} = 0.005,\ \zeta_{40} = 0.0012$
	$B_n = 780.0$	$\zeta_1 = 0.31,\ \zeta_{10} = 0.03,\ \zeta_{40} = 0.007$
beam 1	$B_1 = 2.7,\ B_4 = 43.6,\ B_{14} = 534.3$	$\zeta_n = 0.005$
	$B_1 = 16.4,\ B_4 = 261.9,\ B_{14} = 3205.7$	$\zeta_n = 0.005$
	$B_n = 44.0$	$\zeta_1 = 0.08,\ \zeta_4 = 0.005,\ \zeta_{14} = 0.0004$
	$B_n = 262.0$	$\zeta_1 = 0.48,\ \zeta_4 = 0.03,\ \zeta_{14} = 0.0024$

considered and calculations carried out at 200 uniformly spaced frequencies within this range. Modal summation bandwidths of 16000 rad s^{-1} for the rod systems and 100000 rad s^{-1} for the beam systems were used throughout.

The effects of changing the damping model on the *deterministic* spectra of the dissipated power (i.e. for $\epsilon = 0$) are examined in figures 3 and 4 for the case of rod systems. The extrema observed in the spectra given in these figures are governed not only by the subsystem natural frequencies but also by the mode shapes at the points of driving and coupling. Notice that the spectra of the driven subsystems given here

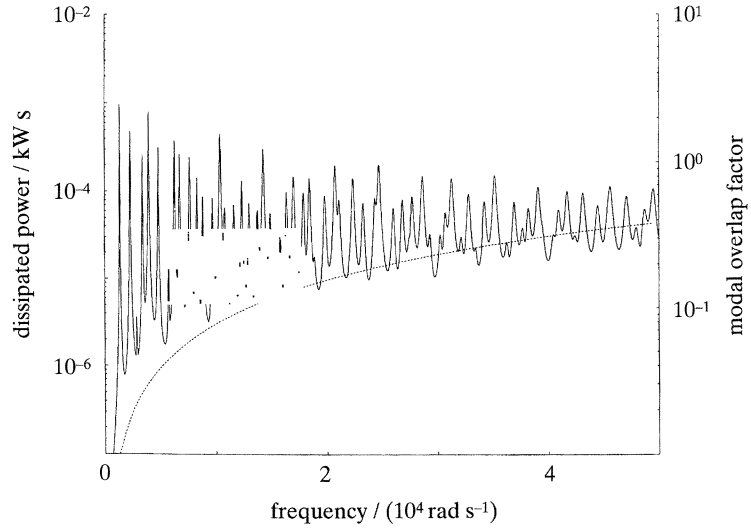

Figure 4. Dissipated power spectral density function for subsystem 1 of the rod system; rain-on-the-roof excitation; $\zeta = 0.005$; key as in figure 3.

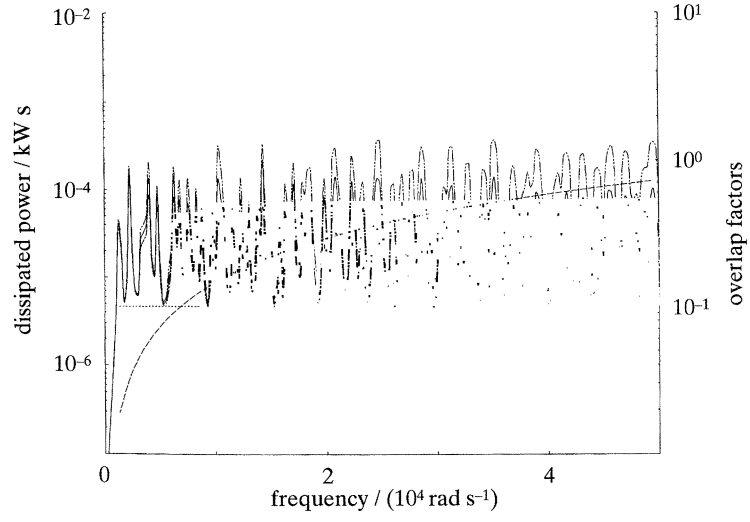

Figure 5. Statistics of the dissipated power spectral density function for subsystem 1 of the rod system; rain-on-the-roof excitation; $\epsilon = 0.01$; $c = 130\ \mathrm{s}^{-1}$; ——, mean; —·—·—, 5% probability point; —··—··—, 95% probability point; ----------, model overlap factor; ————, statistical overlap factor.

are influenced by the natural frequencies of the non-driven subsystems and also by the mode shapes at the points of coupling, these effects being indicative of the strong coupling between the two subsystems. With the constant bandwidth damping model, the modal overlap factor remains constant with respect to frequency and, accordingly, the range of the spectra also remains constant (i.e. the maximum minus the minimum values). Beam systems with constant damping bandwidths behave similarly but the increasing modal spacing reduces the modal overlap factor as the driving frequency rises and, in consequence, the range widens with these increases. For the constant damping ratio model, the modal overlap factor increases with

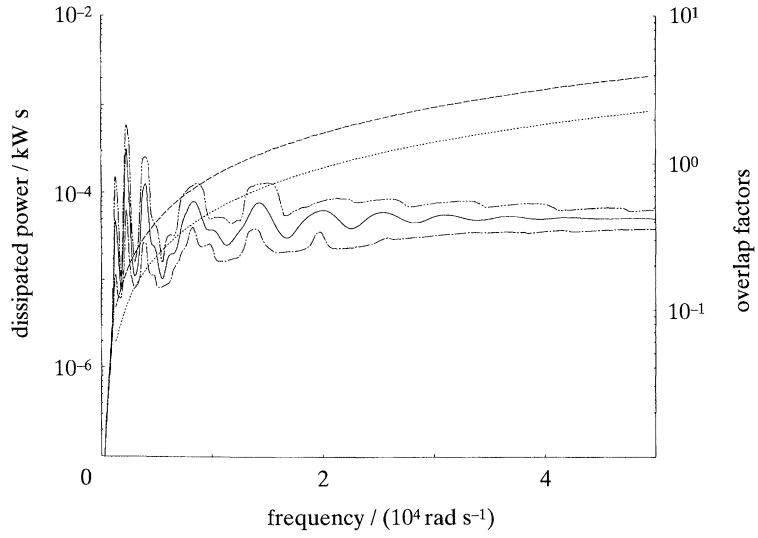

Figure 6. Statistics of the dissipated power spectral density function for subsystem 1 of the rod system; point harmonic excitation; $\epsilon = 0.10$; $\zeta = 0.03$; key as in figure 5.

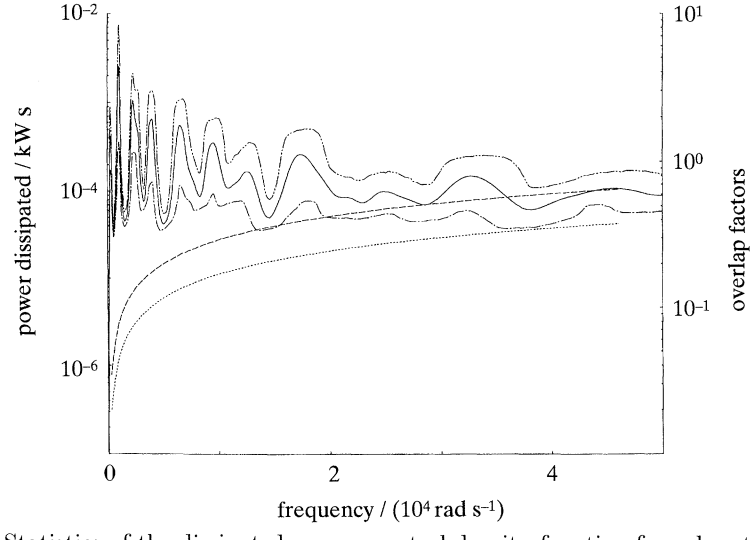

Figure 7. Statistics of the dissipated power spectral density function for subsystem 1 of the beam system; rain-on-the-roof excitation; $\epsilon = 0.10$; $\zeta = 0.03$; key as in figure 5.

frequency for both beams and rods. Consequently, the spectra in such cases tend to become smooth at higher frequencies. Clearly, for all cases, the range is found to reduce with increases in the value of modal overlap factor.

The *statistics* of the response spectra have been estimated using Monte Carlo simulation procedures with 2500 samples and results obtained for the parameter variations mentioned above. A subset of these results are presented in figures 5–12 which display the principal features of the spectral statistics with respect to the different parameters explored. In all cases only the power dissipated in the driven subsystem is plotted: as has already been noted this quantity depends on both the input of energy and its transmission to the undriven subsystem; for the strong

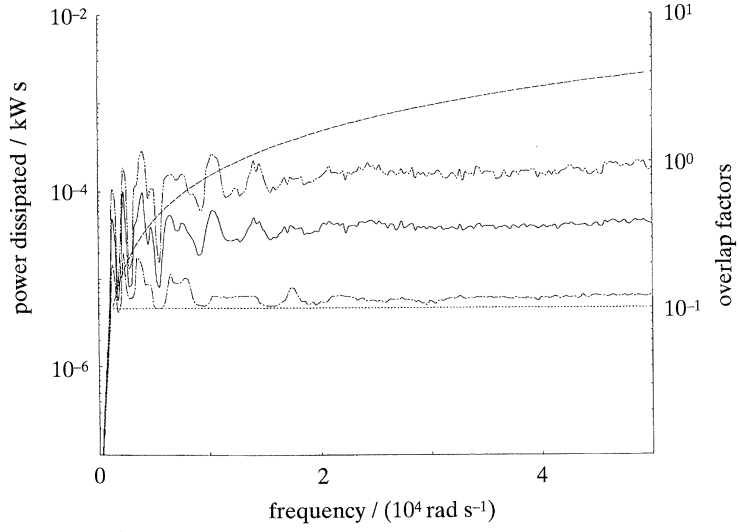

Figure 8. Statistics of the dissipated power spectral density function for subsystem 1 of the rod system; rain-on-the-roof excitation; $\epsilon = 0.10$; $c = 130\ \mathrm{s}^{-1}$; key as in figure 5.

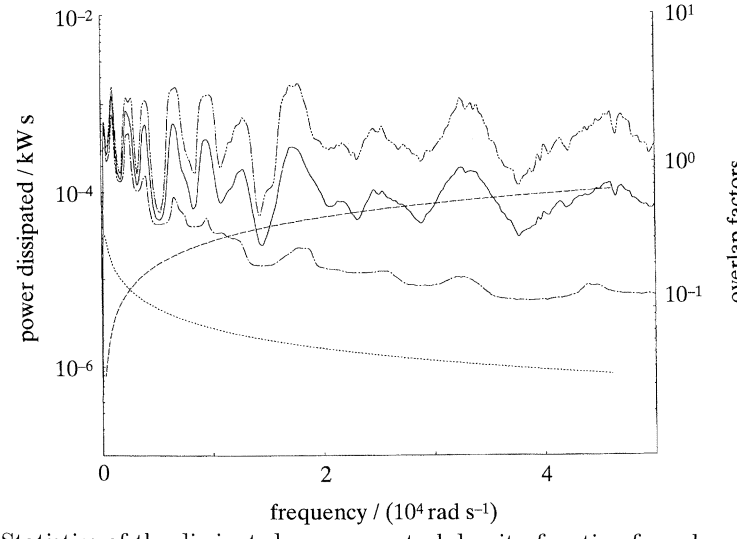

Figure 9. Statistics of the dissipated power spectral density function for subsystem 1 of the beam system; rain-on-the-roof excitation; $\epsilon = 0.10$; $c = 262\ \mathrm{s}^{-1}$; key as in figure 5.

coupling strengths used here these quantities are of roughly equal magnitude and their statistical properties are found to be similar.

1. For low values of ϵ, the trends of the statistics closely follow the corresponding deterministic cases (cf. figures 3 and 5), which is consistent with the fact that, as $\epsilon \to 0$, the statistical solution converges to the corresponding deterministic result. The variability in the response is seen from figure 5 to be greater at higher driving frequencies and this is consistent with the greater variability found in the higher natural frequencies.

2. The most dramatic qualitative change in the behaviour of the 5% and 95% probability points is caused by the choice of damping model. For the constant ζ_n model, the contours of the probability points tend to converge onto the mean for

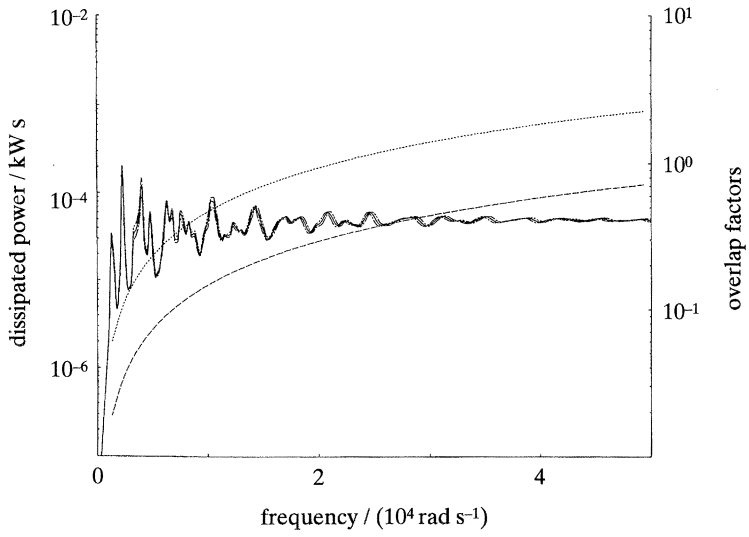

Figure 10. Statistics of the dissipated power spectral density function for subsystem 1 of the rod system; rain-on-the-roof excitation; $\epsilon = 0.01$; $\zeta = 0.03$; key as in figure 5.

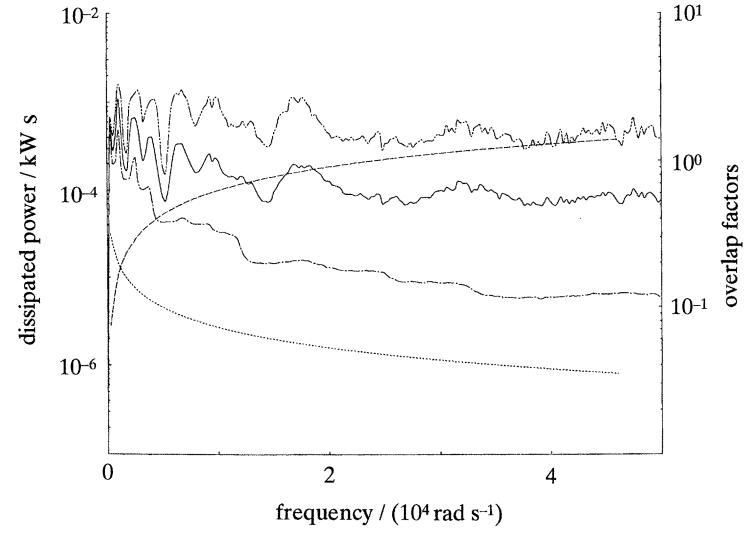

Figure 11. Statistics of the dissipated power spectral density function for subsystem 1 of the beam system; rain-on-the-roof excitation; $\epsilon = 0.20$; $c = 262$ s^{-1}; key as in figure 5.

both the cases of rod and beam systems (figures 6 and 7). This behaviour is associated with increases in the modal overlap factor arising from increases in bandwidth with driving frequency, with the convergence being faster for systems with greater modal overlap factor. On the other hand, for constant B_n, the probability points tend to become constant for rod systems (figure 8), while for beam systems they tend to slowly diverge (figure 9). Again, this behaviour is linked to that of the model overlap factor, which in this case remains constant for rods but reduces with increases in driving frequency for beams.

3. When ϵ is small and the damping heavy, not only is there no great variation between ensemble members, there is also little variation from frequency to frequency,

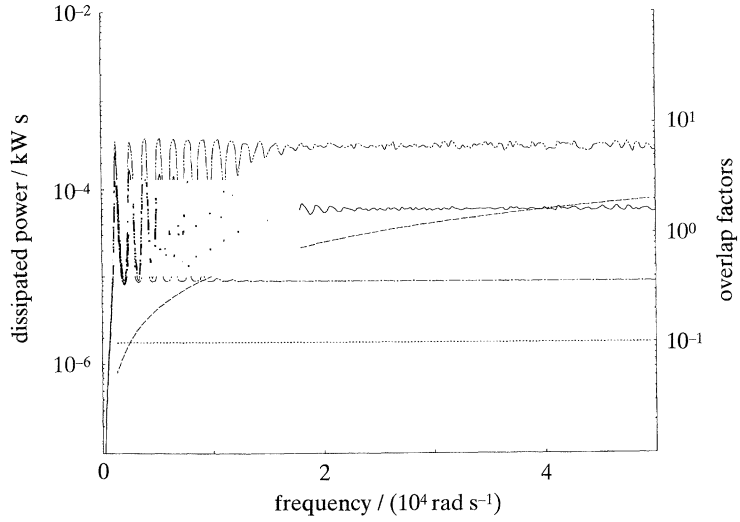

Figure 12. Statistics of the dissipated power spectral density function for rod 1 when it is *uncoupled* from rod 2; rain-on-the-roof excitation; $\epsilon = 0.05$; $c = 130\ \mathrm{s}^{-1}$; key as in figure 5.

since there are then no significant resonant peaks either. In such cases the 5% and 95% points and the mean all tend to constant values with respect to frequency, see figure 10.

4. The frequency beyond which the mean becomes stationary (non-oscillatory) reduces with increases in system randomness (cf. figures 5 and 8). The oscillatory behaviour of the power spectra is caused by two effects, namely, the occurrence of resonances and the variation of mode shape values at the points of coupling (and driving for point forcing). Clearly, in an SEA context, the frequency beyond which the effects of individual natural frequencies and mode shapes cease to dominate variations in the mean value is of considerable interest. A useful criterion for identifying this frequency can be stated in terms of the statistical overlap factor. This survey has shown that for systems under rain-on-the-roof type excitations, choosing a frequency beyond which S_n is greater than 2 guarantees steady mean behaviour (figures 5 and 8). For systems under point forcing, where the mode shapes at the driving point also enter the calculations, S_n needs to be greater than 3 for steady mean behaviour. It may be noted in this context that for the beam systems covered by this survey the statistical overlap factor never reaches such values and therefore the corresponding mean values always remained oscillatory (figures 7 and 9). If ϵ is increased to 0.20, S_n does then become high enough and the mean becomes steady for $S_n > 2$, see figure 11. It may also be noted in this context that the cutoff value of S_n is dependent on coupling strength and is smaller for weakly coupled systems. This point is illustrated in figure 12, where the power dissipated in rod 1, when it is uncoupled from the second subsystem, is shown (i.e. $k_c = 0$). In this case it is seen that $S_n > 1$ is sufficient to guarantee smooth mean behaviour. This is indicative of the fact that the variations in spectra caused by mode shape effects persists longer than those due to resonance effects.

5. For the same level of damping, larger ϵ implies smoother statistics, with the width of the confidence band reaching an upper limit (figures 9 and 11). This feature is more clearly seen in figure 13 which shows the statistics of power dissipated in the beam system under rain-on-the-roof excitation at $\omega = 25000\ \mathrm{rad\ s}^{-1}$, as a function of

ϵ. Clearly, when ϵ is large enough the response at any given frequency may vary all the way from a resonance to an anti-resonance and the 5% and 95% points are then directly related to the bounds of the deterministic spectra. This points towards the usefulness of the study of bounds of the power spectra for connected systems in the context of SEA response variability. In particular, a study of the statistics of the bounds on the spectra would be of interest. Note however, that the models studied here do not exhibit mode shape variations as the mass densities are always taken to be constant along the lengths of the subsystems. In situations where this is not the case, the bounds of the deterministic spectra can no longer be relied upon in this way (see Keane & Manohar 1993). It should also be noted that ϵ is greater than 0.1 before such behaviour is seen in figure 13, corresponding to a normalized standard deviation in the subsystem masses of 10%. This limiting value of ϵ was observed to be smaller for higher values of the driving frequency and subsystem modal overlap factors. On the other hand, for a given level of ϵ, greater damping was seen to result in narrower confidence bands.

6. For the constant bandwidth model, the contour of 5% probability reaches steady state faster than the contour of 95% probability (figures 5 and 8). This feature arises because the peak responses are caused by resonant behaviour and therefore, these responses can be expected to be dominated by a single mode. Conversely, the minimum responses occur at frequencies away from the resonances and therefore, where more than one mode contributes to such responses. At higher driving frequencies the overlap in the PDFs of the natural frequencies increases and the response, even at resonances, will have contributions from several neighbouring modes. This eventually leads to the stationarity of the PDF as a whole.

5. Empirical distribitions

The simulation procedure used to carry out the survey described in the preceding section is general in scope and estimates for the moments and probability distribution functions of the response power spectra can be obtained with equal ease. However, to obtain reliable estimates of the 5% and 95% probability points, a large sample size needs to be used in simulation work. In practical contexts, such large samples are seldom available and decisions often need to be made with a more limited data, where the direct estimates of 5% and 95% probability points will not be sufficiently accurate. Thus, it is desirable to develop empirical procedures to estimate these probability points using knowledge of the first few moments, which, perhaps can be estimated with relatively less difficulty. Clearly, this is a form of curve fitting and its success depends upon the choice of the PDF used to fit the data. It may be noted in this context that the nonlinear nature of the transformations of random variables implicit in equations (1)–(11) rules out the use of analytical procedures for determining the PDFs of the power spectra. Besides, the expressions for the spectra, especially for higher values of k_c, do not easily suggest any limiting distributions which might arise as $\omega \to \infty$ or as the number of terms contributing to the modal summations becomes large. Consequently, the choice of the distribution function has to be based on trial and error procedures and be guided by mathematical and computational expediency.

The experience gained by us in this context has shown that distributions with one parameter, such as the Rayleigh and exponential distributions, do not fit the data well. Amongst distributions with two parameters, the gaussian distribution was

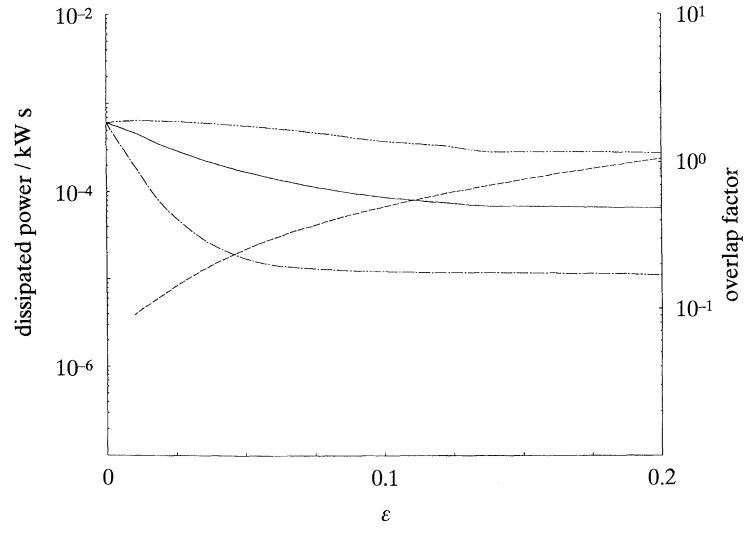

Figure 13. Statistics of the dissipated power spectral density function for subsystem 1 of the beam system; rain-on-the-roof excitation; $\omega = 25000$ rad s^{-1}; $c = 262$ s^{-1}; ——, mean; —·—·—, 50% probability point; —··—··—, 95% probability point; – – – – – –, statistical overlap factor.

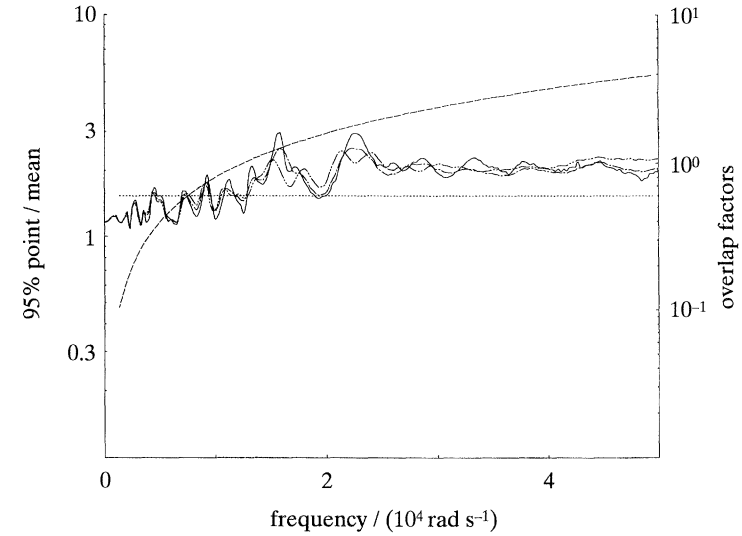

Figure 14. Empirical predictions for the 95% probability point of the dissipated power spectral density function for subsystem 1 of the rod system; point harmonic excitation; $\varepsilon = 0.10$; $c = 780$ s^{-1}; ——, simulated; —·—, gamma; —··—, lognormal; – – – – –, modal overlap factor; ——, statistical overlap factor.

found to be unsuitable, while, the lognormal and gamma distributions give reasonably good fits. To assess the usefulness of these empirical distributions in describing the data, the predictions for the 5% and 95% probability points, skewness and kurtosis coefficients, as functions of ω, were compared with the corresponding simulated results. Two of the predictions for the 95% probability points are shown in figures 14 and 15. Additionally, comparisons of the probability distribution functions at a fixed driving frequency of 40000 rad s^{-1} have been given

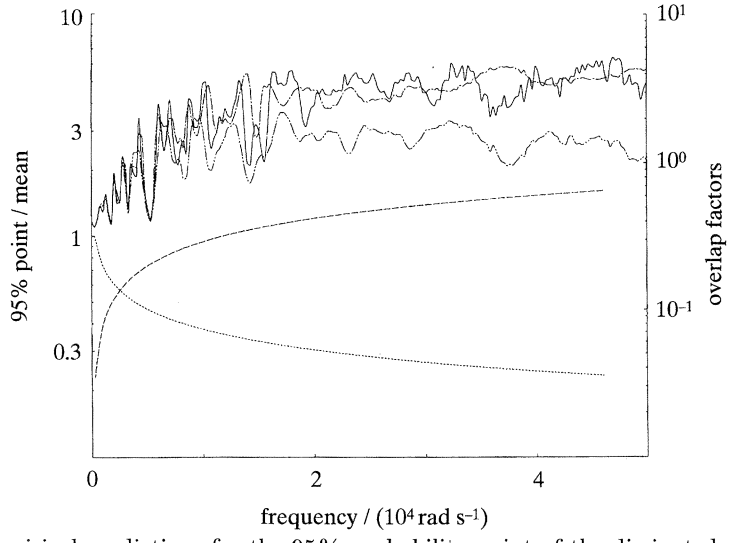

Figure 15. Empirical predictions for the 95% probability point of the dissipated power spectral density function for subsystem 1 of the beam system; rain-on-the-roof excitation; $\epsilon = 0.10$; $c = 262\ s^{-1}$; key as in figure 14.

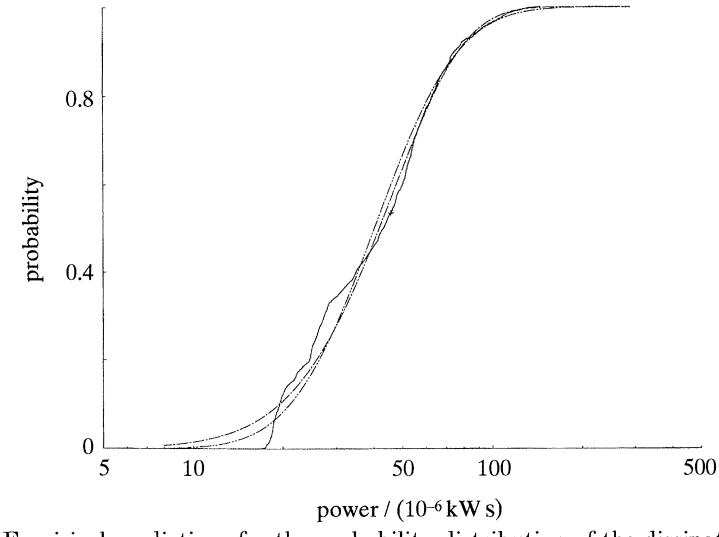

Figure 16. Empirical predictions for the probability distribution of the dissipated power spectral density function for subsystem 1 of the rod system; point harmonic excitation; $\omega = 40000$ rad s^{-1}; $\epsilon = 0.10$; $c = 780\ s^{-1}$; ——, simulated; —·—, gamma; —··—, lognormal.

in figures 16 and 17. A study of these figures reveals that both the gamma and lognormal distributions provide fairly accurate estimates for the 95% probability points, although where the statistical overlap factor is low, the gamma distribution seems to give better results (with the kurtosis and skewness coefficients being generally better predicted). Conversely, the lognormal distribution works better for the 5% points.

As has already been stated, the choice of gamma and lognormal distribution in this study is arbitrary. It may be recalled that the lognormal distribution generally arises as a limiting distribution of products of independent random variables. On the other

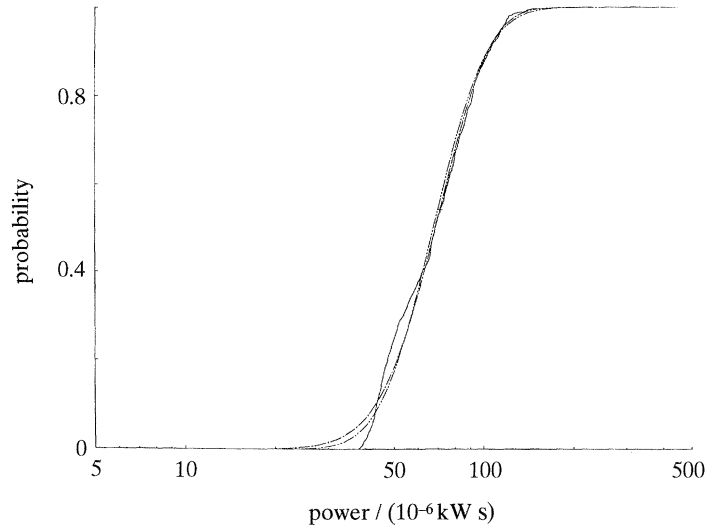

Figure 17. Empirical predictions for the probability distribution of the dissipated power for subsystem 1 of the beam system; rain-on-the-roof excitation; $\omega = 40000$ rad s^{-1}; $\epsilon = 0.10$; $\zeta = 0.03$; key as in figure 16.

hand, the gamma distribution arises in Poisson process theory as the time required for the nth success (see Benjamin & Cornell 1970). Obviously, there is no indication in the expressions for the power spectra (equations (1)–(10)) that the conditions favourable to the existence of either distribution are satisfied. Further work clearly needs to be done to place the use of these distributions on a firmer basis.

6. Conclusions

This study has considered the probability distributions of the dissipated power spectra in a system of two, spring-coupled, one-dimensional subsystems. The effects of changing various parameters of the problem on the behaviour of the PDFs of the response spectra have been studied using Monte Carlo simulation procedures. These changes have encompassed choice of subsystem type, damping model, strength of system randomness and type of excitation (an earlier study considered various classes of subsystem randomness (see Keane & Manohar 1993)). The present work pays particular attention to the choice of damping model and the strength of system randomness. The effects of these quantities have been characterized in terms of the modal overlap factor and a newly introduced statistical overlap factor, S_n. The modal overlap factor takes into account the effect of subsystem type and damping while the statistical overlap factor reflects details of the system randomness.

The work presented shows that a cutoff frequency beyond which the mean response spectra become stationary can be determined by reference to the statistical overlap factor. For the cases considered here, systems driven by point harmonic forcing have mean responses independent of frequency when S_n is greater than 3, while for rain-on-the-roof excitations S_n need only be greater than 2. For systems with weak coupling, it turns out that the above conditions can be relaxed to $S_n > 2$ and $S_n > 1$. This study has also demonstrated that driving frequency dependent variations in the 5% and 95% probability points are strongly influenced by corresponding variations in the modal overlap factor. For rod systems with constant

bandwidth damping models, where the modal overlap factor remains constant with driving frequency, the probability points tend to a constant spacing. For beam systems with constant bandwidth damping models, where the model overlap factor reduces with frequency, the probability points are observed to slowly diverge from each other. Conversely, for constant ζ_n damping models, where the modal overlap factors for both rod and beam systems rise with increases in driving frequency, the probability points converge towards the mean.

In summary, it may be said that, if the modal and statistical overlap factors are both large (> 3, say), the responses of ensemble members tend to show moderate deviations from the mean while the mean remains sensibly independent of driving frequency (e.g. significant damping and parameter randomness, see figure 6). If only the modal overlap factor is large, there will be small deviations from the mean and little variation from frequency to frequency (e.g. significant damping with little parameter randomness, see figure 10). Conversely, if only the statistical overlap factor is large, the 5% and 95% probability points tend to be widely spaced but again the mean tends not to vary much from frequency to frequency (e.g. light damping with significant parameter randomness, see figure 8). Finally, if neither overlap factor is large, although the 5% and 95% points may not be widely spaced the mean is likely to show violent variations from frequency to frequency (e.g. light damping with small parameter randomness, see figure 5). It is usually this last case that is of most interest in structural dynamics and so, since both overlap factors can vary with frequency, precise knowledge of their behaviour would seem to be a precursor to the successful application of SEA methods. Unfortunately, although typical modal overlap factors may be found from a single realization of a problem, the statistical factor requires information from a potentially large population. This may well be available from the output of industrial production lines; it is less easy to derive when dealing with complicated built up structures made in small batches. In the absence of such data the maximum and minimum values observed in the spectra of a single realization may be used to *approximate* the 5% and 95% confidence limits for the ensemble across the range of frequencies surrounding such points; however, such an approach will tend to place the 5% and 95% points further from the mean than is likely in most real structures. Moreover, they will be unable to reflect situations where unusual mode shapes may arise, such as in nearly periodic structures. Alternatively, the 5% and 95% probability points may be estimated using knowledge of the first two moments of the response based on a small sample of systems and an assumed probability function. Preliminary investigations have shown that the lognormal and gamma probability distributions can usefully be used for this purpose, although questions still remain on justifying the choice of these distributions.

This work was supported by funding from the U.K. Department of Trade and Industry which is gratefully acknowledged.

References

Benjamin, J. R. & Cornell, C. A. 1970 *Probability, statistics and decision for civil engineers.* New York: McGraw-Hill.

Craik, R. J. M., Steel, J. A. & Evans, D. I. 1991 Statistical energy analysis of structure-borne sound transmission at low frequencies. *J. Sound Vib.* **144**, 95–107.

Davies, H. G. 1973 Random vibration of distributed systems strongly coupled at discrete points. *J. acoust. Soc. Am.* **54**, 507–515.

Davies, H. G. & Wahab, M. A. 1981 Ensemble averages of power flow in randomly excited coupled beams. *J. Sound Vib.* **77**, 311–321.

Davies, H. G. & Khandoker, S. I. 1982 Random point excitation of coupled beams. *J. Sound Vib.* **84**, 557–562.

Fahy, F. J. & Mohammed, A. D. 1992 A study of uncertainty in applications of SEA to coupled beam and plate systems, part I: Computational experiments. *J. Sound Vib.* **158**, 45–67.

Heron, K. 1990 The development of a wave approach to statistical energy analysis. *Proc. IOA* **12**, 551–555.

Hodges, C. H. & Woodhouse, J. 1986 Theories of noise and vibration transmission in complex structures. *Rep. Prog. Phys.* **49**, 107–170.

Keane, A. J. 1992 Energy flows between arbitrary configurations of conservatively coupled multimodal elastic subsystems. *Proc. R. Soc. Lond.* A **436**, 537–568.

Keane, A. J. & Manohar, C. S. 1993 Energy flow variability in a pair of coupled stochastic rods. *J. Sound Vib.* **168**, 253–284.

Lin, Y. K. 1967 *Probabilistic theory of structural dynamics.* McGraw-Hill.

Lyon, R. H. 1969 Statistical analysis of power injection and response in structures and rooms. *J. acoust. Soc. Am.* **45**, 545–565.

Lyon, R. H. 1975 *Statistical energy analysis of dynamical systems: theory and applications.* MIT Press.

Lyon, R. H. & Eichler, E. 1964 Random vibration of connected structures. *J. acoust. Soc. Am.* **36**, 1344–1354.

Scharton, T. D. & Lyon, R. H. 1968 Power flow and energy sharing in random vibration. *J. acoust. Soc. Am.* **43**, 1332–1343.

Skudrzyk, E. 1968 *Simple and complex vibratory systems.* Pennsylvania State University Press.

Skudrzyk, E. 1980 The mean value method of predicting the dynamic response of complex vibrators. *J. acoust. Soc. Am.* **67**, 1105–1135.

Skudrzyk, E. 1987 Understanding the dynamic behaviour of complex vibrators. *Acoustica* **64**, 123–147.

Soong, T. T. & Bogdanoff, J. L. 1963 On the natural frequencies of a disordered linear chain of N degrees of freedom. *Int. J. mech. Sci.* **5**, 237–265.